lubricants

Article

Measurement and Prediction of Sawing Characteristics Using Dental Reciprocating Saws: A Pilot Study on Fresh Bovine Scapula

Dedong Yu [1,†], Fan Zou [2,†], Wenran Zhang [1,†], Qinglong An [2,*] and Ping Nie [3,*]

1 Department of Second Dental Center, National Clinical Research Center for Oral Diseases, National Center for Stomatology, Shanghai Ninth People's Hospital, College of Stomatology, Shanghai Jiao Tong University School of Medicine, Shanghai Jiao Tong University, Shanghai 201999, China
2 School of Mechanical Engineering, Shanghai Jiao Tong University, Shanghai 200240, China
3 Center of Cranio-Facial Orthodontics, Department of Oral and Cranio-Maxillofacial Surgery, National Clinical Research Center for Oral Diseases, National Center for Stomatology, Shanghai Ninth People's Hospital, College of Stomatology, Shanghai Jiao Tong University School of Medicine, Shanghai Jiao Tong University, Shanghai 201999, China
* Correspondence: qlan@sjtu.edu.cn (Q.A.); nieping@alumni.sjtu.edu.cn (P.N.)
† These authors contributed equally to this work.

Abstract: Bone sawing is one of the most common operations during traditional dental and cranio-maxillofacial surgery and training systems based on virtual reality technology. It is necessary to predict and update conditions (including the sawing force, temperature and tool wear) in real time during VR surgical training and surgical simulation. All the specimens used in this study were fresh bovine scapula. The forces and temperatures were measured during the sawing process. Additionally, the thermal conductivity was measured via a laser flash instrument. Response surface methodology (RSM) was adopted to analyze and model the sawing force and sawing temperature. Meanwhile, tool wear was observed using a scanning electron microscope. The regression models of the sawing force and temperature rise under different experimental conditions were acquired. To obtain the minimum force within the recommended parameter ranges of commonly used medical reference parameters for bone sawing, a higher rotational speed combined with a lower feed rate were recommended. When considering the sawing force and temperature rise comprehensively, the rotational speed should not be extremely high (about 13,000 rpm is recommended). Meanwhile, abrasive wear is the main wear mode of saw blades. In order to avoid surgery failure, it is necessary to replace the saw blade in time. The experimental data were confirmed to be scientific and accurate for the predicted models of sawing conditions. To minimize the main cutting force, a feed rate of 40 mm/min combined with a rotational speed of 13,700 rpm is recommended. High cutting temperatures have the potential to cause irreversible tissue damage, so surgeons using dental reciprocating saws need to avoid excessively high-speed gears.

Keywords: bone sawing; sawing force; tool wear; sawing temperature; surgical training; response surface methodology

check for updates

Citation: Yu, D.; Zou, F.; Zhang, W.; An, Q.; Nie, P. Measurement and Prediction of Sawing Characteristics Using Dental Reciprocating Saws: A Pilot Study on Fresh Bovine Scapula. *Lubricants* **2023**, *11*, 441. https://doi.org/10.3390/lubricants11100441

Received: 29 August 2023
Revised: 23 September 2023
Accepted: 27 September 2023
Published: 12 October 2023

1. Introduction

Osteotomy is an essential segment during bone surgery for orthopedic and craino-maxillofacial surgery. In orthognathic surgery, including Le Fort I osteotomy, bilateral sagittal split ramus osteotomy, genioplasty, etc., the surgeon cuts maxilla or mandible as planned and moves to designed position in order to establish an ideal occlusal relationship and an aesthetic jaw shape. A micro reciprocating saw is widely applied in clinical practice. It is more precise and leads to less bone loss than traditional drills and saws. Meanwhile, maxilla and mandible are anatomically complex, containing abundant nerves and blood vessels compared to long bones. Therefore, the micro reciprocating saw is well suited for the osteotomy of the jaws.

Bone sawing is also a vital procedure in dental and craino-maxillofacial training systems based on virtual reality (VR) technology. The VR training system should be sufficiently realistic to perfectly imitate orthognathic surgery. A high-quality VR training system can train novice physicians to improve technical proficiency. The sawing procedure should minimize force and temperature rise to avoid or alleviate interference with the surgeon and the incidence of complications. Therefore, high-precision models of the sawing force and sawing temperature are becoming increasingly important for VR surgical training and surgical simulations [1–3].

Bone sawing is a process that causes tissue injury. To improve the safety of orthognathic surgery and avoid medical accidents, the reduction of damage during surgery is one of the main goals of related research [4]. The damage mainly arises due to two reasons. One is the stress damage caused by the cutting force [5]. A large mechanical stress will produce microcracks in the bone tissue and even lead to inflammation [6]. The other reason is the thermal damage caused by the sawing temperature [7]. Excessive cutting heat can accelerate the osteonecrosis of bone tissue cells, resulting in the loss of the regeneration function of the bone tissue [8]. Moreover, an inappropriate sawing force and temperature may destroy the surgical instruments and hinder patient recovery [9]. Therefore, accurate prediction and control of the sawing condition are critical to ensure the quality of surgical operation. The material removal mechanism is an important part of research in material machining [10]. The material removal mechanism of bone materials has also been widely studied.

To date, several researchers have made endeavors to develop sawing force prediction models, most of which have been based on material properties and mechanical models. Scholars have investigated methods for modeling cutting temperature and cutting force, including linear regression models, multiple regression models and neural network methods. James [11] et al. proposed a new sawing force model based on the concept of a single tool sawing at a depth of cut less than the cutting edge radius to predict bone sawing forces. Other studies have mainly focused on the establishment of a regression model of the sawing force [12]. Lin [13] et al. established a sawing force model for virtual surgery training based on virtual reality (VR) technology.

According to relevant studies, the overall rate of instrument breakage during surgery has been 0.35% [14]. It is dangerous for a saw blade to fail during surgery. The wear performance of common materials has been extensively studied [15–17]. The failure mechanism of the saw blade is also an essential research topic that is studied to avoid potential risks. Many studies have focused on the wear phenomenon and mechanism of bone drill [18–20]. However, to date, few studies have been reported that address the wear mechanism of a saw blade used to cut bone material. Additionally, the prediction of the sawing force is the main focus of researchers, and the existing sawing force models fail to take the anisotropy of bone materials into consideration. Moreover, the cutting temperature and tool wear are still not well understood.

In the current work, a precisely controlled experimental platform with various measurement functions was established to conduct sawing experiments. Stryker thin blades, which are commonly used in osteotomy, were utilized. Based on the experimental data, regression models of the sawing force and sawing temperature were established. Response surface methodology (RSM) was used to analyze the influence of sawing parameters on the sawing force and sawing temperature. In addition, the wear signatures of the sawing blades were observed and analyzed to reduce the risk of surgical tool failure. The models established in the current work can help to realize haptic feedback and surgical simulation, which contributes to orthognathic surgical training based on VR technology.

The sawing test was carried out on a specially designed experimental platform to determine the optimal parameters of the bone saw. Meanwhile, according to the experimental data, the model can be used for VR training.

2. Materials and Methods

2.1. Measurement of Thermal Diffusivity

The thermal diffusivity of cortical bone and cancellous bone was measured with a laser flash instrument (type NETZSCH LFA 467, Selb, Germany). In the measurement of the cortical bone thermal diffusivity, the orientations parallel to the osteons and perpendicular to the osteons were considered. The specimen was machined using a precision cutting machine with a size of 10 mm × 10 mm × 1 mm. The temperature of the specimen in the test was slowly increased from 0 °C to 100 °C, and the thermal diffusivity was measured at 10 °C intervals.

2.2. Sawing Experiments on Fresh Bovine Scapula

The specimens used in this study were provided by a slaughterhouse. Soft tissues were removed from the scapula, and the specimens were preserved in saline solution for experimentation. All the experiments were approved by the Ethics Committee of Shanghai Ninth People's Hospital.

The sawing experiments were conducted on a specially designed experimental platform, as shown in Figure 1. The experimental platform is fixed on a five-axis machining center (DMG, type DMU60, Stuttgart, Germany) with a position accuracy of 0.01 mm to realize precise motion control. The bone was firmly clamped by a specially designed fixture upon a Kistler dynamometer (KISTLER, type 9267, Winterthur, Switzerland), which can capture the in situ force signals generated during the sawing process. A temperature measuring system with an infrared thermal imager (FLIR, type A615, Wilsonville, OR, USA) was used to monitor and record the temperature signal in the sawing test. A fresh saw blade (STRYKER, type 5100-137-134, Portage, MI, USA), which is often used in orthognathic surgery, was utilized in the sawing experiments. The details of the saw blade are shown in Figure 2.

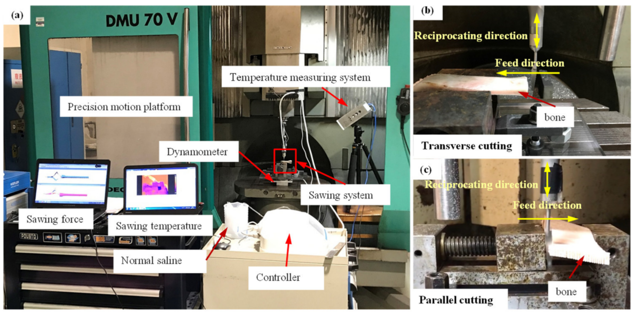

Figure 1. Experimental setup. (**a**) Sawing and measurement system, (**b**) Schematic diagram of transverse cutting, (**c**) Schematic diagram of parallel cutting.

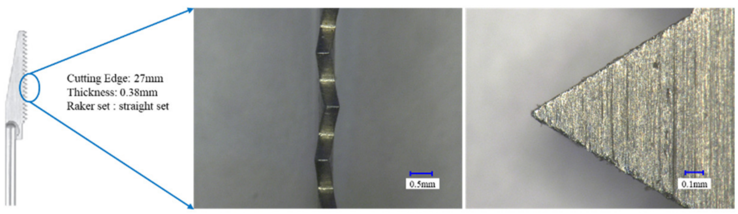

Figure 2. Saw blades used in the experiment.

In the current work, the feed rate and rotation speed were set as the main research variables. In addition, the angle between the saw blade and the osteons may influence the force and temperature. As summarized in Table 1, a full factorial experiment with 24 sawing conditions was designed; among the sawing conditions, "parallel" means that the sawing direction was parallel to the direction of the osteons, and "vertical" means that the sawing direction was perpendicular to the direction of the osteons.

Table 1. Sawing Test Parameters.

No.	Sawing Type	Feed Rate (mm/min)	Rotation Speed (r/min)
1	Parallel	40	9800
2	Parallel	60	9800
3	Parallel	80	9800
4	Parallel	40	11,200
5	Parallel	60	11,200
6	Parallel	80	11,200
7	Parallel	40	12,600
8	Parallel	60	12,600
9	Parallel	80	12,600
10	Parallel	40	14,000
11	Parallel	60	14,000
12	Parallel	80	14,000
13	Vertical	40	9800
14	Vertical	60	9800
15	Vertical	80	9800
16	Vertical	40	11,200
17	Vertical	60	11,200
18	Vertical	80	11,200
19	Vertical	40	12,600
20	Vertical	60	12,600
21	Vertical	80	12,600
22	Vertical	40	14,000
23	Vertical	60	14,000
24	Vertical	80	14,000

For reliability of the experimental results, three repeated tests were carried out under each cutting condition, and the result used in the analysis was the average of the results of the three tests.

2.3. Flow Chart of This Work

Figure 3 shows the flow chart of this work. The study was divided into three parts: sawing experiments, measurements and observations, analysis and optimization. The cutting force and cutting temperature were measured in situ in the bone sawing experiment, and the tool was observed after the test. The measured data were processed and analyzed, and a multiple regression model was used to fit the model of cutting force and temperature variation with parameters. The sawing parameters were also optimized.

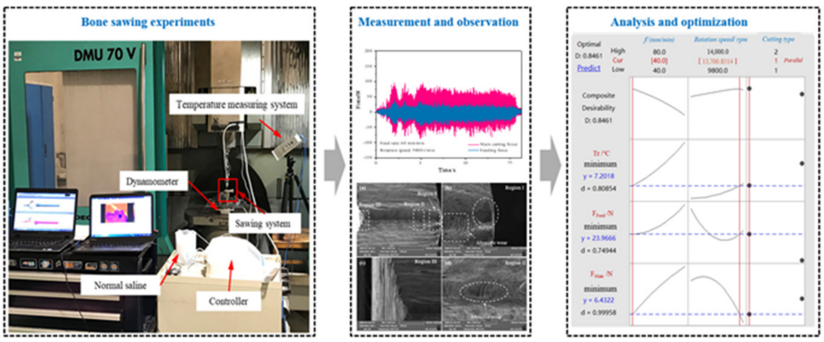

Figure 3. Flow Chart of This Work.

2.4. Modeling of Sawing Condition to Realize VR Surgical Training

Response surface methodology (RSM) was adopted to model the sawing force and temperature rise in the sawing procedure of fresh bovine scapula specimens. Response surface methodology is a collection of statistical and mathematical techniques used for the purpose of setting up a series of experiments for adequate predictions of a response and for fitting a hypothesized model to data obtained under the chosen design. Main effects and potential secondary effects can be identified by the RSM method. Meanwhile, the results of multi-objective optimization can also be obtained.

The general form of the multivariable regression formula can be expressed as Equation (1).

$$y = \beta_0 + \sum_{i=1}^{k} \beta_i x_i + \sum_{i=1}^{k} \beta_{ii} x_i^2 + \sum_{i} \sum_{j} \beta_{ij} x_i x_j + \varepsilon \quad (1)$$

where y is the response variable; β_0 is a constant; $\beta_1, \beta_2, \ldots, \beta_k$ are coefficients; $x_1, x_2, \ldots, x_k$ are the input variables and ε is an error term.

By inputting the sawing force model into the VR surgical training equipment, the magnitude and direction of the sawing force can be calculated in real time. Then, the real-time updated calculation results will be fed back to the operator through the force feedback handle until the operation is completed.

2.5. Observation of the Wear Characteristics of Saw Blades

The failure of the saw blade is detrimental to orthognathic surgery. An observation of the wear characteristics of saw blades is helpful to avoid such risks. After the tests, the saw blades were treated by ultrasonic cleaning for 5 min in acetone, and the wear characteristics of the cutting edges were rigorously investigated via a scanning electron microscope (TESCAN, type VEGA 3, Brno, Czech). TESCAN VEGA3 is a thermionic emission SEM system that comes either with a tungsten heated filament or lanthanum hexaboride (LaB_6) as the electron source.

3. Results

Before the sawing trials, the thermal diffusivity of the cortical bone and cancellous bone were measured, and the acquired results are shown in Figure 4. The thermal diffusivity of the cortical bone and cancellous bone fluctuated within the range of 0~100 °C, and the thermal diffusion coefficient parallel to the direction of the osteons was the greatest. It can be seen that the variation of thermal diffusivity of the bone materials fluctuated less in the range of 0~100 °C between 0.1–0.175. The thermal diffusivity of the cortical bone was significantly higher than that of the cancellous bone. The thermal diffusivity of the cortical bone parallel to the osteon direction was slightly higher than that perpendicular to the cortical bone direction. Figure 4 shows the morphology of the bone material and machined surface after the experiment. As shown in Figure 5a, the distance between each sawing trace was greater than 1 mm to reduce the interaction effect. The cutting traces could be observed on the machined surface of the bone material.

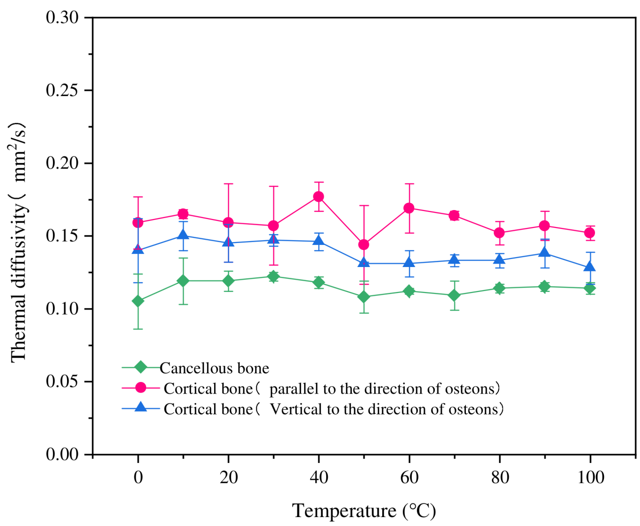

Figure 4. Measurement of the thermal diffusivity of the bone materials.

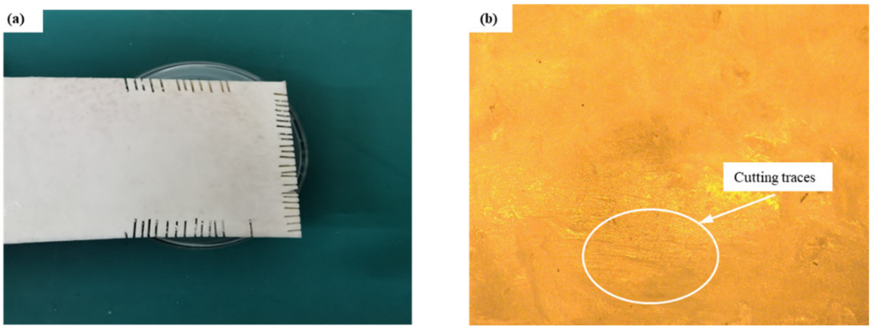

Figure 5. (**a**) Bone material after sawing and (**b**) a sawed surface.

The cutting force and temperature under different cutting parameters were obtained during the sawing process. Figure 6a is a schematic diagram of the sawing process, where the main cutting force is along the reciprocating direction of the saw blade, and the feed force is along the tool feed direction. The typical cutting force signal is shown in Figure 5b. The frequency of the cutting force signal was consistent with the reciprocating motion of the tool. The average values of the main sawing forces and feed forces under different cutting conditions are depicted in Figures 7 and 8. The main cutting force decreased with the increase in rotating speed and increased with the increase in the feed force. The variation trend of the feed force with sawing parameters was similar to that of the main cutting force. The evolution of the temperature rise with different cutting parameters is illustrated in Figure 9, and a scanning electron microscopy (SEM) image showing the wear signatures of the saw blade is shown in Figure 10. The experiment was carried out to observe the tool as a whole and focused on the wear in the cutting edge region. The worn blade was sawed 200 mm in length with the parameter of feed rate: 40 mm/min and rotation speed: 13,700 rpm.

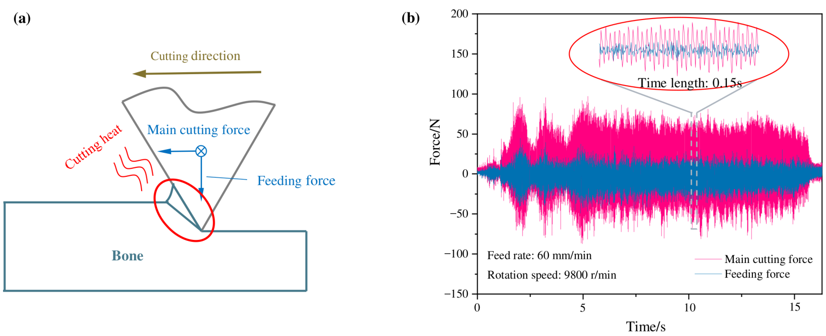

Figure 6. (**a**) Typical cutting force signal and (**b**) schematic diagram of the sawing process.

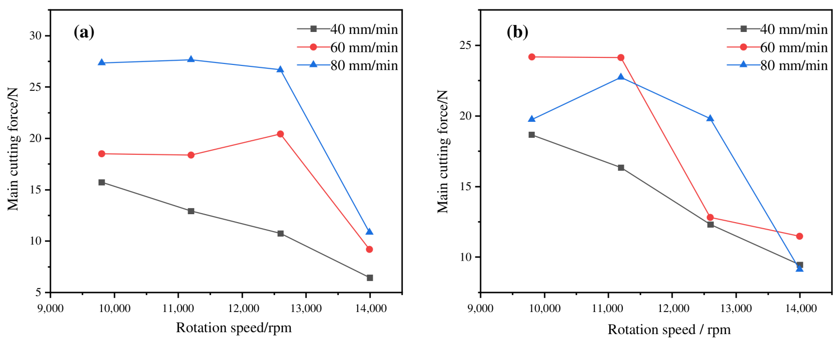

Figure 7. The main cutting force with different experimental parameters: (**a**) parallel sawing and (**b**) vertical sawing.

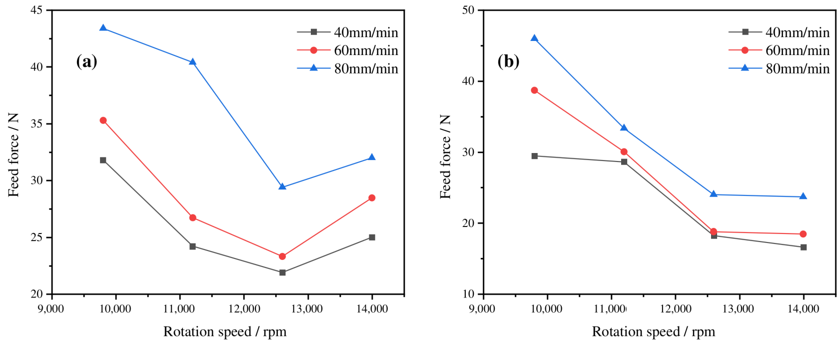

Figure 8. The feed sawing force with different experimental parameters: (**a**) parallel sawing and (**b**) vertical sawing.

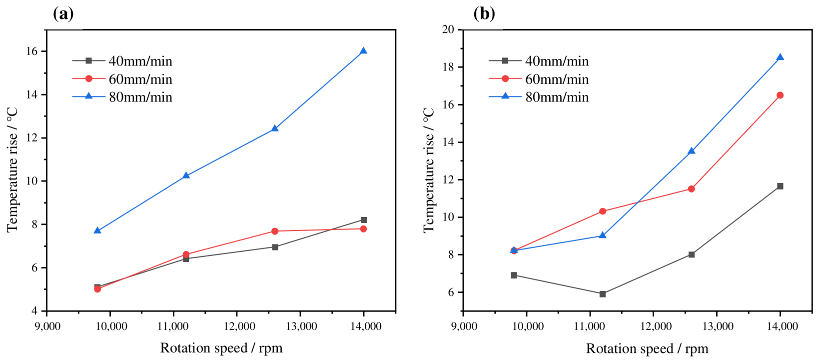

Figure 9. The temperature rise with different experimental parameters: (**a**) parallel sawing and (**b**) vertical sawing.

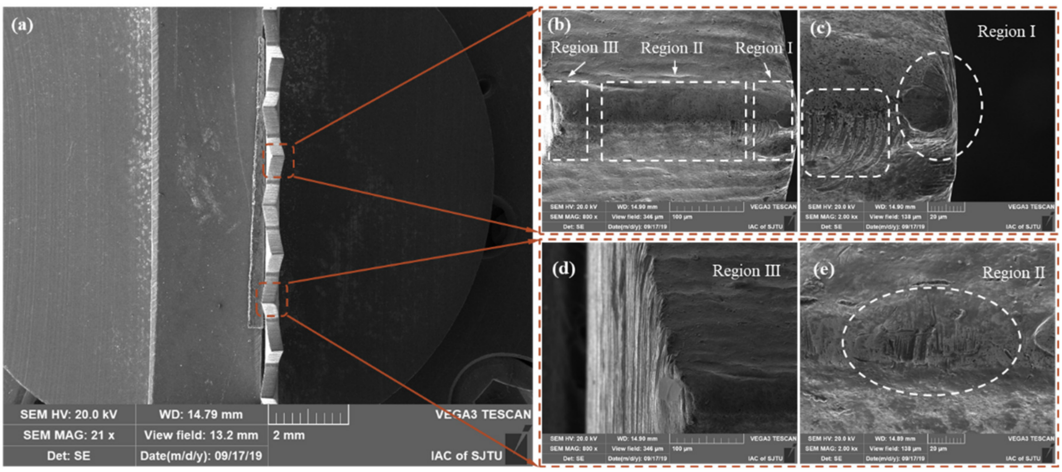

Figure 10. Observation of the wear characteristics of the saw blades. (**a**) Macro morphology of saw blades, (**b**) Wear characteristics of saw blade tooth tip, (**c**) Wear characteristics of the bottom part of the saw blade teeth. (**d**) Wear characteristics of the bottom part of the saw blade teeth, (**e**) Wear mechanism of the bottom part of the saw blade teeth.

According to Equation (2), cutting depths in this paper can be obtained. The cutting depth can be calculated as follows:

$$D_c = 500f/n \quad (2)$$

where D_c is the depth of the cut, f is the feed rate and n is the rotation speed.

According to Equation (2), the cutting depths under different cutting parameters are summarized in Table 2.

Table 2. Cutting depth under different cutting parameters.

Parameters	Value								
f (mm/min)	40	40	40	60	60	60	80	80	80
n (r/min)	9800	11,200	12,600	9800	11,200	12,600	9800	11,200	12,600
D_c (μm)	2.04	1.78	1.59	3.06	2.68	2.38	4.08	3.57	3.17

Multiple regression models of the sawing force and sawing temperature were established based on the acquired force and temperature signals. Full quadratic formulas were introduced to express the variation in the main cutting force, feed force and temperature rise, as shown in Equations (3)–(5), respectively. The multiple regression model is widely used for modeling cutting temperatures and cutting forces [21], including those of bone materials [22]. It has the advantages of fast computation and high applicability. The model is commonly used for force feedback in virtual surgical systems [23].

$$\begin{cases} F_{Main} = -122.4 + 0.763f + 0.02112v - 0.00183f^2 - 0.000001v^2 - 0.000021f \times v \quad (P) \\ F_{Main} = -180.0 + 0.562f + 0.02090v - 0.00183f^2 - 0.000001v^2 - 0.000021f \times v \quad (P) \end{cases} \tag{3}$$

$$\begin{cases} F_{Feed} = 171.0 + 0.261f - 0.02477v + 0.00444f^2 + 0.000001v^2 - 0.000044f \times v \quad (P) \\ F_{Feed} = 201.0 + 0.210f - 0.02728v + 0.00444f^2 + 0.000001v^2 - 0.000021f \times v \quad (P) \end{cases} \tag{4}$$

$$\begin{cases} T_{Rise} = 31.9 - 0.407f - 0.00377v + 0.00167f^2 + 0.000001v^2 + 0.000028f \times v \quad (P) \\ T_{Rise} = 29.5 - 0.439f - 0.00324v + 0.00167f^2 + 0.000001v^2 + 0.000028f \times v \quad (P) \end{cases} \tag{5}$$

where “P” indicates that the sawing direction is parallel to the direction of the osteons, and “V” signifies that the sawing direction is perpendicular to the direction of the osteons.

Within the scope of the current experiment, the accuracy of the developed models is acceptable. The analysis of the residual plot and the normal probability plot of the residuals was another effective method used to estimate the accuracy of the established models [24]. Figure 11 shows that the normal probability plots of the residuals reflect approximately straight lines, which verifies that the residuals are normally distributed, and that the regression results are fitted well. The effects of the experimental parameters (feed rate and rotation speed) on the sawing force and temperature are discussed for sawing bone materials. Figures 12–14 show contours corresponding to the minimax response surface, which was obtained using the RSM method. The contours depict the behavior of the force and temperature with the interaction effects from the input variables based on the full quadratic formulas. To obtain a lower cutting force and temperature, higher rotational speeds and lower feed rates are preferred.

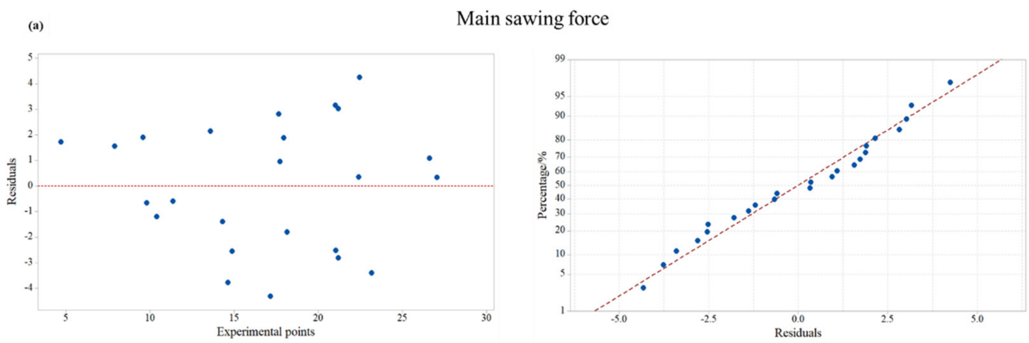

Figure 11. *Cont.*

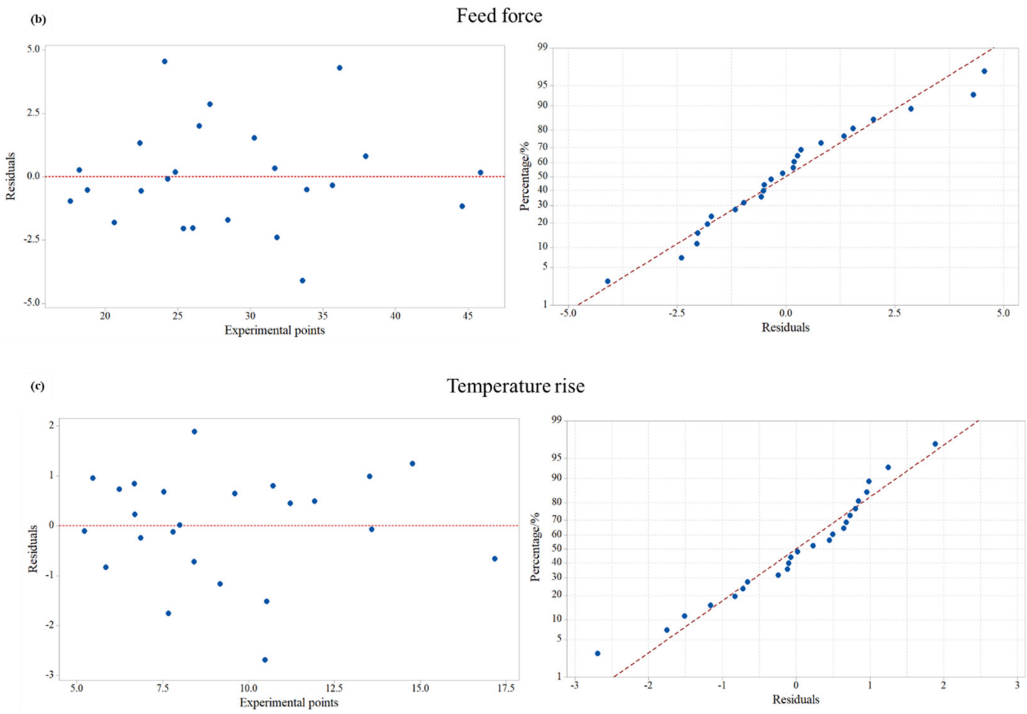

Figure 11. Residual fitted values for the models and experimental results, and their expectations assuming a normal distribution: (**a**) main cutting force; (**b**) feed force; (**c**) temperature rise.

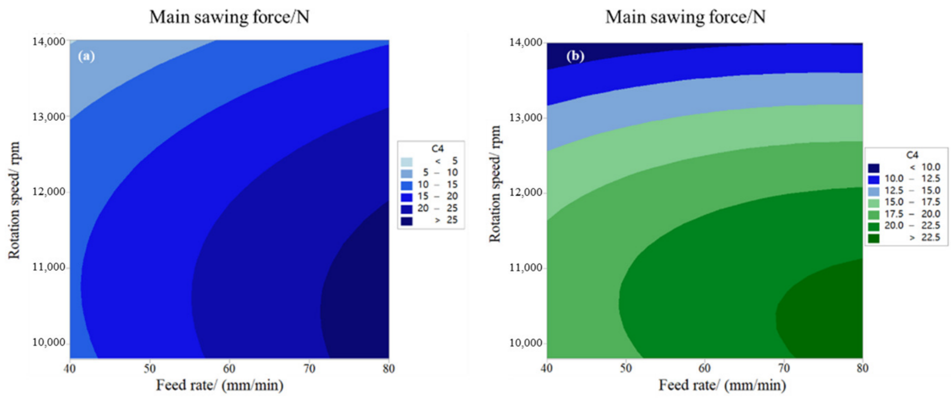

Figure 12. The effects of the sawing parameters on the main cutting force (**a**) parallel sawing and (**b**) vertical sawing.

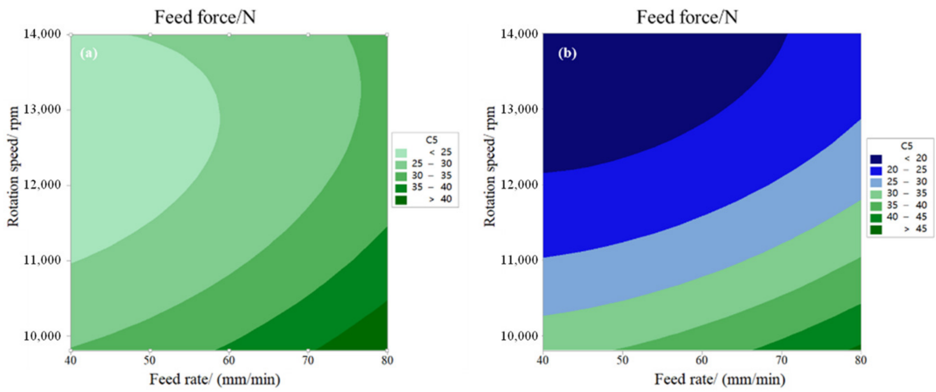

Figure 13. The effects of the sawing parameters on the feed force. (**a**) parallel sawing and (**b**) vertical sawing.

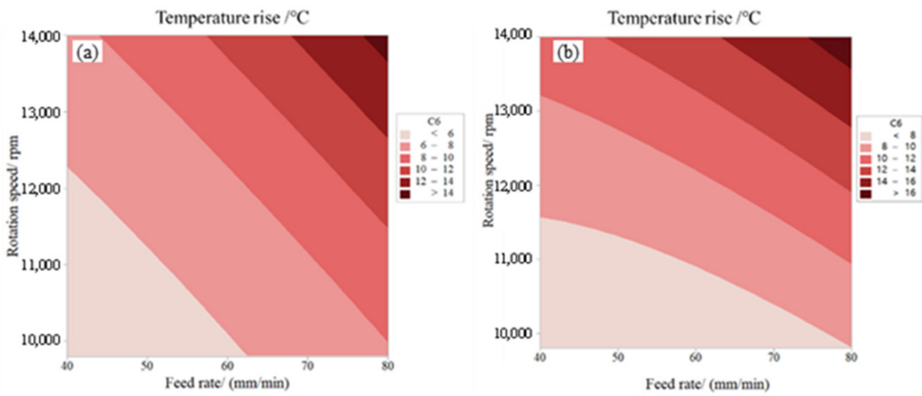

Figure 14. The effects of the sawing parameters on the temperature rise. (**a**) parallel sawing and (**b**) vertical sawing.

4. Discussion

Potential intraoperative adverse events in orthognathic surgery include abnormal hemorrhage due to infection or injury, fracture and split, osteonecrosis, etc. [25]. The mandible is identified as adverse-event-prone, probably due to its unique anatomical conditions, such as its masticatory muscle attachment, articulatory function, difficulties in visualizing the inferior alveolar neurovascular bundle and strict demands for osteotomy and fixation [26]. Therefore, it is necessary to optimize the procedure comprehensively in order to minimize the incidence of adverse events. In this study, we analyzed the sawing force, sawing temperature and the wear signatures of the sawing blades, targeting a set of sawing parameters standard for both safety and efficiency.

In most studies, the temperature measured in the experiment is used as the index of sawing temperature. However, the temperature rise is more suitable as an evaluation index because there is a difference between the experimental temperature (usually at room temperature) and the operating temperature. Meanwhile, it needs to be determined that the thermal diffusivity of the bone material changes with temperature. Information about the thermal diffusivity of bone materials at different temperatures cannot be found in the existing literature. Bone material is a typical heterogeneous anisotropic material. Directionality should be considered. The thermal diffusivity of the cortical bone and cancellous bone change slightly, within the range of 0~100 °C. This indicates that the temperature rise (*Tr*) can be used to evaluate the temperature during bone material sawing.

During surgery, the cutting force is one of the most important indexes used to evaluate the sawing process, and it affects the control accuracy and structural tissue damage. There is a negative correlation between the main cutting force and rotation speed. Meanwhile, the main cutting force has a positive correlation with the feed rate. The variation in the feed force with the different sawing parameters is similar to that of the main cutting force. However, when the speed reaches 14,000 rpm, the feed force exhibits an accelerating trend.

Previous studies have shown that excess heat in the bone could lead to irreversible damage or even necrosis when reaching 47 °C [27]. In many procedures, an irrigation channel is added to offset the heat accumulation of the sawing. However, on the one hand, water flow may interfere with the operation view. On the other hand, digital surgical guide plates, which are increasingly clinically popular, could block the water flow from heat transfer with bone tissue, making it difficult to achieve the goal of cooling [28]. Therefore, reducing the heat generated by the saw itself is the fundamental way to reduce the damage. As shown in Figure 9, the sawing temperature shows a positive correlation with the feed rate and rotation speed. During the sawing process, the heat generated by the friction between the saw blade and the bone material is the main contribution to the increase in the cutting temperature. As the rotating speed increases, the heat generated by the friction increases proportionally, which leads to a sharp rise in the sawing temperature. In comparison with the rotating speed, the feed rate has less positive impact on the sawing temperature. In general, the higher the feed rate is, the larger the cutting force and thus the greater the work of friction between the saw blade and the bone material.

According to the related literature [29], the material removal mechanism of the bone is shear cutting at a relatively low cutting depth (less than 20 μm). When the cutting depth exceeds 80 μm, bone chips form from the bone material mainly due to fracturing. Since the cutting mode and crack growth often lead to many very small cracks forming in the bone material, promoting inflammation during healing [30], the cutting mode of shear cutting is recommended in surgery. Therefore, the feed speed must be controlled within a certain range. When cutting at a depth greater than 20 μm, the cutting mode and crack growth often lead to many very small cracks forming in the bone material, promoting inflammation during healing. During surgery, it is necessary to appropriately reduce the feed (moving speed) when the rotational speed decreases. Table 2 shows that the cutting depths are less than 10 μm regardless of the experimental parameters used and can meet the actual requirements of orthognathic surgery. With the cutting mode of shear cutting, the friction coefficient is approximately 0.82 when the cutting direction is parallel to the osteons, and the shear stress (τ_s) is 85 MPa [31]. When the cutting direction is perpendicular to the osteons, the friction coefficient is approximately 0.85 and the resulting shear stress is 191 MPa. This explains why the cutting force and cutting temperature tend to be higher when the cutting direction is perpendicular to the osteons. We consider "perpendicular" and "parallel" to build a more accurate model. This technology can improve the reality of VR training.

With regard to tool wear, abrasive wear is the main wear form of saw blades when cutting such materials. The tool wear is mainly affected by the friction between the high-density minerals in the bone material and the saw blade during the sawing process. Since the sawing temperature and force are low in the bone material, it is difficult to generate other forms of tool wear, such as adhesive wear and diffusion wear.

A higher rotational speed in bone sawing reduces cutting forces and increases cutting temperatures. In surgery, lower cutting forces can reduce the labor intensity of the surgeon to perform the operation more accurately. However, excessive temperatures will lead to irreversible thermal damage to tissues. Therefore, choosing the right speed (taking into account both cutting force and cutting temperature) can help in surgical procedures. With the aim of achieving a minimum sawing force and temperature, the experimental parameters are optimized. Considering the range of commonly used parameters for orthognathic in Table 1, the optimized curve is shown in Figure 15. The minimum main cutting force, feed force and temperature rise are 6.4322 N, 23.9666 N and 7.2 °C with the following optimized parameters: a feed rate of 40 mm/min, a rotational speed of 13,700 rpm and a sawing direction parallel to the osteons. Moreover, in future experiments or surgeries, attention should be paid to replacing saw blades at appropriate intervals and fixing the specimen firmly during sawing.

In addition, the study had several limitations. Firstly, it was an in vitro study using bovine scapulae. The mechanical properties of bovine and human bones are not identical. And heat dissipation occurs in living bodies due to mechanisms such as blood flow, which could not be simulated in our experiments. Secondly, the infrared thermal imager measured temperature changes on the surface, which deviated somewhat from the temperature rise inside the bone. Finally, the parameters derived from our study still need abundant, emulation and probative tests before being applied in clinical practice.

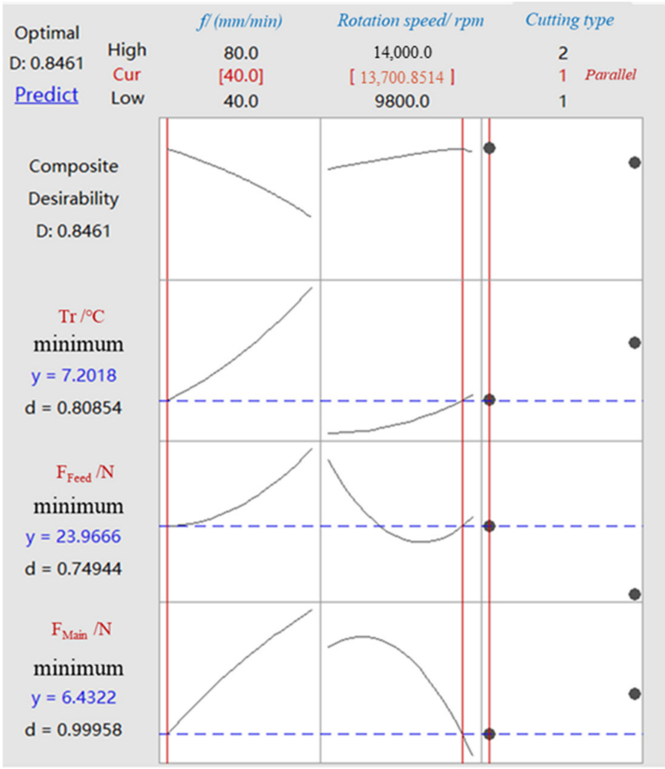

Figure 15. Optimization of the parameters to achieve a minimum sawing force and temperature.

5. Conclusions

This work carried out sawing experiments on bone materials. The changing law of cutting force and cutting temperature was studied, and the mechanism of tool wear was analyzed. Meanwhile, a multivariate regression model capable of being used for virtual surgery training was obtained. The conclusions obtained are as follows.

To minimize the main cutting force, a feed rate of 40 mm/min combined with a rotational speed of 13,700 rpm is recommended. When considering the sawing force and temperature rise comprehensively, the rotational speed should not be extremely high (about 13,000 rpm is recommended). When surgeons use dental reciprocating saws, they need to avoid high-speed gears for reducing thermal damage to tissues. The experimental data were confirmed to be scientific and accurate for the predicted models of sawing condition, which can be used in VR training systems.

Author Contributions: Statement: (1) D.Y., F.Z. and W.Z. were responsible for the design, conducting of the experiments, data collection and drafting of the article, and accountable for all aspects of the work. F.Z., D.Y. and W.Z. contributed equally. (2) P.N. and Q.A. were responsible for the experimental design, data interpretation, critical revision of the article and approval of article. P.N. and Q.A. contributed equally. All authors have read and agreed to the published version of the manuscript.

Funding: This work was funded by the National Natural Science Foundation of China (Grant No. 52175422 and 32101094); Clinical Research Project of Health Industry of Shanghai Health Commission (Grant No. 202240194) and Cross-disciplinary Research Fund of Shanghai Ninth People's Hospital, Shanghai Jiao Tong University School of Medicine (Grant No. JYJC202114).

Institutional Review Board Statement: Not applicable.

Informed Consent Statement: Not applicable.

Data Availability Statement: Not applicable.

Conflicts of Interest: The authors declare no conflict of interest.

References

1. Wu, Y.; Wang, F.; Fan, S.; Chow, J.K.-F. Robotics in Dental Implantology. *Oral Maxillofac. Surg. Clin.* **2019**, *31*, 513–518. [CrossRef] [PubMed]
2. Srivastava, R.; Jyoti, B.; Priyadarshi, P.K. Computer Aided Navigation for Predictable Dental Implantology: A Review. *Natl. J. Integr. Res. Med.* **2019**, *10*, 3.
3. Yan, Y.; Li, Q.; Wang, Q.; Peng, Y. Real-Time Bone Sawing Interaction in Orthopedic Surgical Simulation Based on the Volumetric Object. *J. Vis.* **2018**, *21*, 239–252. [CrossRef]
4. Yu, D.; Liu, C.; Wu, Y.; An, Q. Measurement and Prediction of Drilling Force in Fresh Human Cadaver Mandibles: A Pilot Study. *Clin. Implant Dent. Relat. Res.* **2020**, *22*, 4–12. [CrossRef] [PubMed]
5. Tawy, G.F.; Rowe, P.J.; Riches, P.E. Thermal Damage Done to Bone by Burring and Sawing with and without Irrigation in Knee Arthroplasty. *J. Arthroplast.* **2015**, *31*, 1102–1108. [CrossRef] [PubMed]
6. He, H.; Wang, C.; Zhang, Y.; Zheng, Y.; Xu, L.; Xie, G.; Zhao, D.; Chen, B.; Chen, H. Investigating Bone Chip Formation in Craniotomy. *Proc. Inst. Mech. Eng. Part H J. Eng. Med.* **2017**, *231*, 959–974.
7. Lee, J.; Chavez, C.L.; Park, J. Parameters Affecting Mechanical and Thermal Responses in Bone Drilling: A Review. *J. Biomech.* **2018**, *71*, 4–21. [CrossRef] [PubMed]
8. Reingewirtz, Y.; Szmuklermoncler, S.; Senger, B. Influence of Different Parameters on Bone Heating and Drilling Time in Implantology. *Clin. Oral Implant. Res.* **2010**, *8*, 189–197. [CrossRef]
9. Donath, K. A Method for the Study of Undecalcified Bones and Teeth with Attached Soft Tissues. *J. Oral Pathol. Med.* **1982**, *11*, 318–326. [CrossRef]
10. Liu, H.; Zhao, P.; Guo, Y.; Li, D.; Wang, Y.; Sun, S.; Wu, J. Material removal behaviors of FCC metals in nanoscale and microscale scratching: Theoretical model and experiments. *J. Mater. Process. Technol.* **2023**, *312*, 117855. [CrossRef]
11. James, T.P.; Pearlman, J.J.; Saigal, A. Rounded Cutting Edge Model for the Prediction of Bone Sawing Forces. *J. Biomech. Eng.* **2012**, *134*, 071001. [CrossRef] [PubMed]
12. Hsieh, M.S.; Tsai, M.I.G.-D.A.; Yeh, Y.-D. An Amputation Simulator with Bone Sawing Haptic Interaction. *Biomed. Eng. Appl. Basis Commun.* **2006**, *18*, 229–236. [CrossRef]
13. Conward, M.; Samuel, J. A Microstructure-Based Mechanistic Model for Bone Sawing: Part 1—Cutting Force Predictions. *J. Manuf. Sci. Eng.* **2021**, *143*, 121009. [CrossRef]
14. Pichler, W.; Mazzurana, P.; Clement, H.; Grechenig, S.; Grechenig, W. Frequency of Instrument Breakage During Orthopedic Procedures and Its Effects on Patients. *J. Bone Jt. Surg.* **2009**, *90*, 2652–2654. [CrossRef] [PubMed]
15. Kumaraswamy, J.; Anil, K.C.; Shetty, V.; Shashishekar, C. Wear behaviour of the Ni-Cu alloy hybrid composites processed by sand mould casting. *Adv. Mater. Process. Technol.* **2023**, *9*, 351–367. [CrossRef]
16. Kumaraswamy, J.; Shetty, V.; Sanman, S.; Naik, P.; Shedthi, S.; Gnanavel, C.; Mogose, I.N. Thermal Analysis of Ni-Cu Alloy Nanocomposites Processed by Sand Mold Casting. *Adv. Mater. Sci. Eng.* **2022**, *2022*, 2530707. [CrossRef]
17. Kumaraswamy, J.; Anil, K.C.; Shetty, V. Development of Ni-Cu based alloy hybrid composites through induction furnace casting. *Mater. Today Proc.* **2023**, *72*, 2268–2274. [CrossRef]
18. Allsobrook, O.F.; Leichter, J.; Holborow, D.; Swain, M. Descriptive Study of the Longevity of Dental Implant Surgery Drills. *Clin. Implant Dent. Relat. Res.* **2011**, *13*, 244–254. [CrossRef]
19. Koopaie, M.; Kolahdouz, S.; Kolahdouz, E.M. Comparison of Wear and Temperature of Zirconia and Tungsten Carbide Tools in Drilling Bone: In Vitro and Finite Element Analysis. *Br. J. Oral Maxillofac. Surg.* **2019**, *57*, 557–565. [CrossRef]
20. Queiroz, T.P.; Souza, F.Á.; Okamoto, R.; Margonar, R.; Pereira-Filho, V.A.; Garcia, I.R., Jr.; Vieira, E.H. Evaluation of Immediate Bone-Cell Viability and of Drill Wear after Implant Osteotomies: Immunohistochemistry and Scanning Electron Microscopy Analysis. *J. Oral Maxillofac. Surg.* **2008**, *66*, 1233–1240. [CrossRef]
21. Tahmasbi, V.; Qasemi, M.; Ghasemi, R.; Gholami, R. Experimental study and sensitivity analysis of force behavior in cortical bone milling. *Med. Eng. Phys.* **2022**, *105*, 103821. [CrossRef] [PubMed]
22. Lin, Y.; Yu, D.; Chen, X.; Wang, X.; Shen, G.; Wang, C. Simulation and evaluation of a bone sawing procedure for orthognathic surgery based on an experimental force model. *J. Biomech. Eng.* **2014**, *136*, 034501.
23. James, T.P.; Pearlman, J.J.; Saigal, A. Predictive force model for haptic feedback in bone sawing. *Med. Eng. Phys.* **2013**, *35*, 1638–1644. [CrossRef] [PubMed]
24. Heydari, H.; Kazerooni, N.C.; Zolfaghari, M.; Ghoreishi, M.; Tahmasbi, V. Analytical and Experimental Study of Effective Parameters on Process Temperature During Cortical Bone Drilling. *Proc. Inst. Mech. Eng. Part H J. Eng. Med.* **2018**, *232*, 871–883. [CrossRef] [PubMed]
25. Knoedler, S.; Baecher, H.; Hoch, C.C.; Obed, D.; Matar, D.Y.; Rendenbach, C.; Kim, B.-S.; Harhaus, L.; Kauke-Navarro, M.; Hundeshagen, G.; et al. Early Outcomes and Risk Factors in Orthognathic Surgery for Mandibular and Maxillary Hypo- and Hyperplasia: A 13-Year Analysis of a Multi-Institutional Database. *J. Clin. Med.* **2023**, *12*, 1444. [CrossRef] [PubMed]
26. Zaroni, F.M.; Cavalcante, R.C.; da Costa, D.J.; Kluppel, L.E.; Scariot, R.; Rebellato, N.L.B. Complications Associated with Orthognathic Surgery: A Retrospective Study of 485 Cases. *J. Cranio-Maxillofac. Surg.* **2019**, *47*, 1855–1860. [CrossRef] [PubMed]
27. Eriksson, A.R.; Albrektsson, T. Temperature Threshold Levels for Heat-Induced Bone Tissue Injury: A Vital-Microscopic Study in the Rabbit. *J. Prosthet. Dent.* **1983**, *50*, 101–107. [CrossRef] [PubMed]

28. Liu, Y.-F.; Wu, J.-L.; Zhang, J.-X.; Peng, W.; Liao, W.-Q. Numerical and Experimental Analyses on the Temperature Distribution in the Dental Implant Preparation Area When Using a Surgical Guide. *J. Prosthodont.* **2018**, *27*, 42–51. [CrossRef]
29. Yeager, C.; Nazari, A.; Arola, D. Machining of Cortical Bone: Surface Texture, Surface Integrity and Cutting Forces. *Mach. Sci. Technol.* **2008**, *12*, 100–118. [CrossRef]
30. Augustin, G.; Davila, S.; Mihoci, K.; Udiljak, T.; Vedrina, D.S.; Antabak, A. Thermal Osteonecrosis and Bone Drilling Parameters Revisited. *Arch. Orthop. Trauma Surg.* **2008**, *128*, 71–77. [CrossRef]
31. Liao, Z.; Axinte, D.A. On Chip Formation Mechanism in Orthogonal Cutting of Bone. *Int. J. Mach. Tools Manuf.* **2016**, *102*, 41–55. [CrossRef]